Nuclear Instruments and Methods in Physics Research A 604 (2009) 604–611

Contents lists available at ScienceDirect

Nuclear Instruments and Methods in Physics Research A

journal homepage: www.elsevier.com/locate/nima

Application of the Recursive Subtraction Pulse Shape Analysis algorithm to in-beam HPGe signals

F.C.L. Crespi [a], F. Camera [a,*], A. Bracco [a], B. Million [a], O. Wieland [a], V. Vandone [a], F. Recchia [b], A. Gadea [b], Th. Kröll [b], D. Mengoni [c], E. Farnea [c], C.A. Ur [c], D. Bazzacco [c], the AGATA collaboration

[a] Dipartimento di Fisica, Università di Milano and INFN Sezione di Milano, Via Celoria 16, 20133 Milano, Italy
[b] Laboratori Nazionali di Legnaro, INFN, Viale dell'Università 2, 35020 Legnaro, Padova, Italy
[c] Dipartimento di Fisica, Università di Padova and INFN Sezione di Padova, Via Marzolo 8, 35131 Padova, Italy

ARTICLE INFO

Article history:
Received 15 December 2008
Received in revised form
10 March 2009
Accepted 19 March 2009
Available online 5 April 2009

Keywords:
Gamma-rays
HPGe detectors
Pulse Shape Analysis
AGATA
Tracking

ABSTRACT

The Pulse Shape Analysis algorithm "Recursive Subtraction" has been applied to data acquired during the in-beam tests of two different highly segmented HPGe detectors. This algorithm processes the net charge signal, determining the number of interactions per segment and their radial coordinates. The RS algorithm performances are evaluated by comparing the results obtained following its application to experimental pulse shapes with those obtained with specific GEANT simulations. Excellent agreement is found between the experimental distribution of the number of interactions per segment and the simulated one. Deviations between experimental radial distribution and the calculated ones are discussed.

1. Introduction

High-resolution γ-ray spectroscopy plays a prominent role in the investigation of nuclear structure. Present generation arrays, mainly based on Compton-suppressed High Purity Germanium (HPGe) detectors (EUROBALL [1], GAMMASPHERE [2], EXOGAM [3], JUROGAM [4], RISING [5] and CLARA [6]), have significantly contributed to our understanding of nuclear structure in both high and low spin domain and have allowed to initiate the investigation of the isospin degree of freedom.

However, the presence of BGO shields prevents the 4π solid angle coverage with HPGe detectors, thus limiting the photopeak efficiency of the array to values up to approximately 10–20% [3,7].

In next generation γ-spectroscopy arrays (AGATA [7] or GRETA [8]), the full solid angle will be covered with electrically segmented HPGe crystals. This solution, which removes BGO shields, maximizes the active solid angle and, consequently, the photopeak efficiency. In addition, the electrical segmentation of HPGe crystal gives the possibility to reconstruct the path of each γ-ray inside the detectors (i.e. γ-ray tracking) [7,8]. With this approach, an unprecedented sensitivity will be achieved and the challenging requirements for the γ-ray detection systems to be used in experiments with exotic nuclear beams can be fulfilled. In fact, the γ-ray tracking will allow to correct for the energy shift caused by Doppler effect, recovering the intrinsic HPGe energy resolution, and to reject the background events which do not deposit their full energy inside the array or do not originate from the target position [9,10].

The basic information needed by γ-ray tracking algorithms consists in the spatial position of all the interaction points (IPs) and in the related amount of energy released in the detector. The position sensitivity of the detectors is achieved through the segmentation of the outer contact and by the shape analysis of the measured pulses (PSA). A segmentation level of the crystal that guarantees a maximum of one IP in each electrical segment is unfortunately technically and practically unfeasible in terms of complexity and cost [11]. The required performances of PSA algorithms in terms of position resolution and their impact on γ-ray tracking efficiency was discussed in several papers (see for example [10,12–14]). Presently, a position resolution of the order of 5 mm (FWHM) for the IP coordinates determination is considered realistic and it is used in almost all γ-ray tracking simulations.

Since PSA algorithms are supposed to run on-line, during the data acquisition, they should not overload the CPU as this produces unwanted dead time. Unfortunately, as a general feature, the quality of the results is in open conflict with the CPU requirement especially if one has to disentangle more than one IP in a signal.

* Corresponding author.
E-mail address: camera@mi.infn.it (F. Camera).

0168-9002/$ - see front matter © 2009 Elsevier B.V. All rights reserved.
doi:10.1016/j.nima.2009.03.203

A simple PSA algorithm (Recursive Subtraction, RS) for the identification of the interaction number per segment and of their radial positions was presented by the authors in Ref. [15]. The algorithm is characterized by an average success rate of 85% for simulated γ-ray events at 662 keV. Although the present algorithm does not provide the full positional information, it does provide a key information for the tracking, i.e. the number of interactions in the segment, as well as an accurate determination of their radial coordinates. The RS algorithm can be used stand-alone or coupled to a second PSA algorithm when a full 3D localization of the interaction point is required. A sequence of two algorithms in cascade could enhance the performances of the overall process in terms of both execution time and localization precision. In fact, a main algorithm capable to extract the 3D interaction positions with the needed precision could be preceded by another more simple one that rapidly provides partial information. Indeed, the RS algorithm is designed for this last purpose and examples of PSA methods that would benefit from a fast determination of the number of interactions in a segment are those presented in Refs. [16,17].

In this paper we present the results of the application of the RS algorithm to real pulse shapes acquired during the in-beam tests of two different highly segmented HPGe detectors, namely, a 25-fold segmented HPGe detector denoted with "MARS" [18,19] and the first AGATA symmetric cluster (composed by three 36-fold segmented HPGe detectors) [20,21]. Presently there are several works concerning the PSA analysis on measured pulses [20–29] but, to our knowledge, this is the first application of a PSA algorithm for coaxial HPGe segmented detectors, which fulfils the CPU requirements to run on-line and extracts the number of hits. Therefore the present algorithm was applied to in-beam data to extract the number of interactions per segment and their radial coordinates. Other algorithms exist such as the "GRID SEARCH" described in Refs. [20,21], optimized to provide an efficient Doppler Correction and which gives an accurate localization only for the most energetic IP. Similarly, the results obtained using an in-beam test for a GRETINA detector, reported in Ref. [29], assume that gamma-ray events in a segment consist of two single-site interactions. Also in the Compton Imager with HPGe detectors, with which an impressive spatial resolution was achieved [30–34], single hit events were selected.

Since it is not possible to know a priori the number of IPs per segment and their positions for each event acquired in a real measurement (this is the information that the PSA algorithm is supposed to extract), RS algorithm performances are evaluated by comparing the results obtained following its application to experimental pulse shapes with those extracted using GEANT simulations. The effect of the electric noise and of the finite bandwidth of the pre-amplifier on the calculated signal shape was taken into account [15,35].

The description of the two experiments in which the pulse shapes were acquired is given in Section 2, while results concerning the radial coordinate and IPs number determination are discussed in Section 3. Finally, in Section 4 the discussion on the RS algorithm execution time performances is presented.

2. The in-beam experiments

The signals analyzed with the RS algorithm were acquired during two different experiments. The first one was performed at Legnaro INFN laboratory using the 25-fold segmented coaxial HPGe detector MARS [18–21] (see Fig. 1a), while the second was performed at IKP Koeln using the AGATA symmetric cluster (composed by three 36-fold segmented hexaconically tapered HPGe crystals, see Fig. 1b). Detailed information on both the mentioned in-beam tests can be found in dedicated publications [17–21].

The MARS detector consists of a semi-coaxial n-type HPGe crystal; it has a cylindrical shape with 90 mm length and 72 mm diameter. The inner hole has 10 mm diameter and 75 mm depth. The outer contact is segmented into 25 parts, as shown in Fig. 1a: there are four subdivisions along the detector axis ("slices") and six angular subdivisions ("sectors"). In addition a small segment is positioned at the centre of the detector front face (this is labeled with an F in Fig. 1a). In the in-beam test of MARS detector a coulomb excitation reaction of ^{56}Fe accelerated at 240 MeV on ^{208}Pb target was used. Following the transition between the first excited state and the ground state of ^{56}Fe a 846.8 keV γ-ray is emitted. The detector was positioned at 16 cm distance from the target and at an angle of 135° with respect to the beam direction, which corresponds to 90° with respect to the direction of the recoils detected using an array of pin diode detectors. The data acquisition system (DAQ) was composed by an array of seven digital oscilloscopes LeCroy LT244 [19,36]. These oscilloscopes have four channels, a sampling rate of 200 MSamples/s and

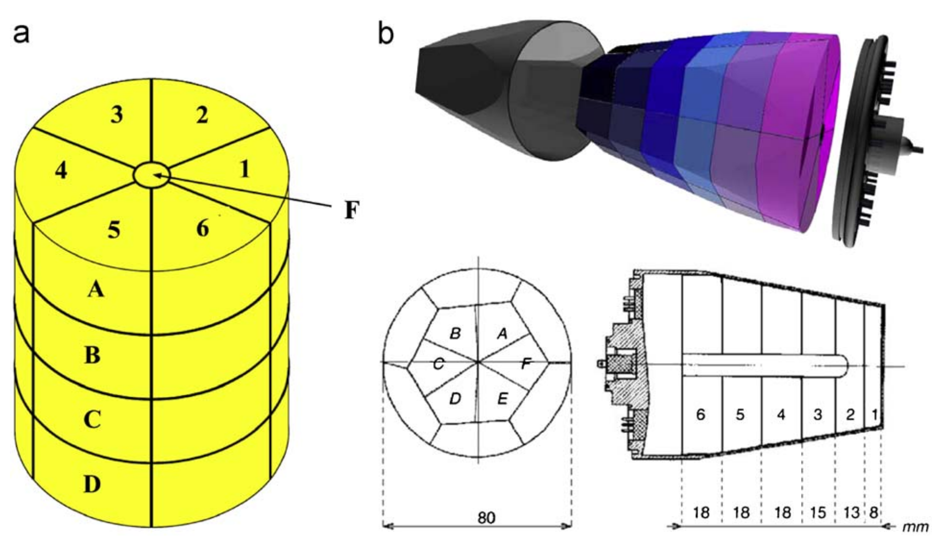

Fig. 1. (a) Layout of the HPGe MARS detector segmentation. (b) Schematic view of the 36-fold segmented, hexaconically tapered HPGe crystal of AGATA. The segmentation pattern is reported. The figures are taken from Refs. [19,21].

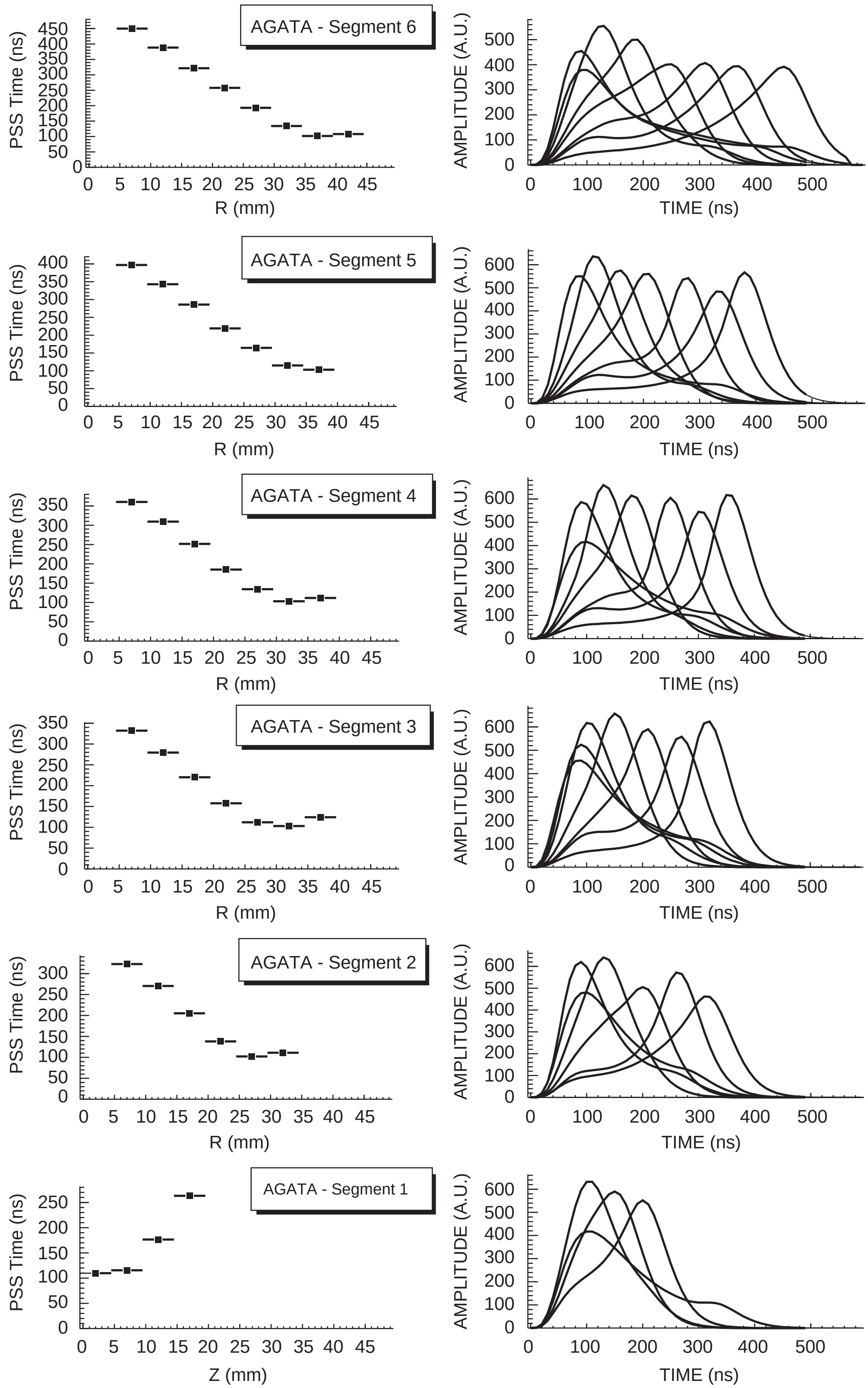

Fig. 2. Right column: current pulse shapes calculated for different radial position of the gamma interaction inside the AGATA detector volume. All the signals exhibit the typical peak shaped structure (PSS). Each panel refers to a different AGATA detector segment. The segment number is the same as the one of Fig. 1 and each segment is representative of one detector slice (6 in total). Left column: for each simulated current pulse the PSS maximum position is plotted as a function of the radial (z in the first segment) coordinate of the gamma interaction point.

a resolution of 8 bits. The data have been pre-processed (as accurately described in Ref. [19]) in order to time-align the pulses and extract the energy released in each detector segment. For each acquired event the amount of energy released (calibrated, in keV) and the traces (each consisting of 2002 samples for a time interval of about 1 μs) are given.

In the analysis of the data, only the events in which the whole 846.8 keV γ-ray energy was released in a single segment belonging to the quasi-true coaxial part of the detector were selected. This choice was taken in order to use the signal basis calculated in the simplest possible situation. In fact, in this case, deviations in the radial coordinate determination due to the non-coaxial symmetry of the detector are avoided. In addition, the selection of events which fully deposit their energy in a single segment enhances the average number of IPs per segment and, consequently, makes more stringent the test of the algorithm.

The AGATA symmetric cluster is composed by three 36-fold segmented n-type HPGe detectors. Each HPGe crystal (see Fig. 1b) has an hexagonal front face of dimensions 61.1×52.9 mm extending backwards with a tapering angle of 10°; when the hexagon reaches a diameter of 80 mm the crystal has cylindrical geometry. The inner hole has a diameter of 10 mm. The total length of the crystal is 90 mm. The AGATA symmetric cluster in-beam experiment was performed using the tandem accelerator in IKP Koeln. The reaction used was ^{48}Ti(d, p)^{49}Ti at beam energy of 100 MeV. Following the transition between the first excited state and the ground state of ^{49}Ti a 1381.7 keV γ-ray is emitted. The data acquisition system was based on GSI MBS [5,37]. The germanium signals were digitized using XIA-DGF modules (14 bits, 40 MSamples/s) and consist of 20 samples for a total sampling time of 500 ns; these cards provide also a measured value of the net charge deposited inside each segment. In this measurement the AGATA cluster was placed at about 10 cm from the target and at an angle of 90° with respect to the beam axis. The scattered protons of the (d, p) reaction were measured using an annular DSSSD detector. The acquired signals were first preprocessed and time aligned by means of a digital CFD as described in Ref. [21]. As for the experiment with the MARS detector, also for the analysis of the AGATA cluster data only the events in which the whole γ-ray energy was released in a single segment were selected. However, in this case, the analysis was not restricted to segments belonging to the quasi-true coaxial part of the detector.

3. Pulse Shape Analysis with RS algorithm

One of the basic assumptions of the RS algorithm is the existence of a direct relation between the current pulse maximum position and the spatial localization of the interaction [15]. The validity of this assumption was already verified in Ref. [15] for both MARS and AGATA crystals, but only in the coaxial part of the detectors. It is therefore important to assure the validity of this assumption for the whole volume, especially in the front-end part. For this purpose the plots in the left column of Fig. 2 show the relation between the spatial localization of the interaction and the current pulse maximum position in the signals (displayed in the right column of Fig. 2) from the MGS calculated basis [38,39] for an AGATA crystal. The MGS_v5-r2 version was used to produce the signals of Fig. 2 and for the analysis described in the following sections as well. Each panel of Fig. 2 is associated to a detector segment representative of one slice. All the graphs show the current pulse peak maximum position plotted against the radial coordinate of the interaction. The only exception is for the bottom panel (corresponding to the front-end segment) in which the z coordinate is chosen. This is because of the geometry of the front-end part of the detector. As can be seen from the figure, in all the segments, current pulses corresponding to different radial/(z) coordinate can be easily identified through the position of the maximum and its width.

As already discussed in Ref. [15] the RS algorithm is characterized by a parameter (which here we name "NIT") that defines the multiplicity of the signals considered to represent the first decomposed interaction. As was shown in Ref. [15] the algorithm performances can be enhanced increasing the value of this parameter, at the expense of CPU time. Furthermore, it was shown that for values of NIT > 50 the RS algorithm performances do not increase significantly. Following these argumentations and the fact that for NIT = 50 the execution time of the algorithm is still significantly under 1 ms (see Section 4), it has been chosen to set NIT = 50 for the processing of all the simulated and experimental data presented in this work.

In all the presented data, for the determination of the number of IPs (from here denoted as IPn), the RS algorithm makes use of an important assumption that two disentangled interactions having the associated pulse shape maxima in the same radial position are counted as one. This assumption, discussed in Ref. [15], was used since two signals, with the maxima exactly in the same radial position, give rise, in most of the cases, to a signal shape identical to that of one single interaction event, which is more likely to happen.

3.1. Radial coordinate determination

In this section, the results obtained using the RS algorithm for the determination of radial coordinate are described. In particular, the RS algorithm performances are evaluated by comparing the radial distribution of the events reconstructed by PSA with that resulting from GEANT simulations. This is the only way to verify the reliability of RS Pulse Shape Analysis technique when applied on experimental signals. In fact, for the acquired events, it is not possible to know a priori, on an event-by-event basis, the number of interactions per segment and their radial coordinate.

Fig. 3 shows the comparison between the radial distribution of the IPs measured in the experiment with the MARS detector (extracted using the RS algorithm) and the simulated one [40].

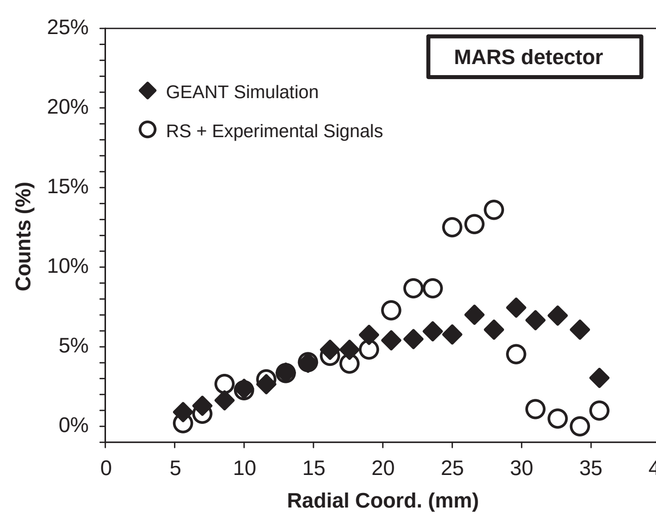

Fig. 3. The radial coordinate distribution of the most energetic gamma interaction, obtained applying the RS algorithm to the experimental signals acquired during the MARS experiment, is reported with empty black circles. This is compared with the expected one, obtained with a GEANT simulation of the MARS experiment [40] (filled black diamonds). As can be clearly seen, the experimental distribution well reproduces the simulated one up to $R = 2$ cm, then it deviates in the outer part of the detector ($2 < R < 3.5$ cm).

The distributions, displayed in the figure, are both normalized to 1. As can be clearly seen, the experimental distribution well reproduces the simulated one up to $R = 2$ cm, then it deviates in the outer part of the detector ($2<R<3.5$ cm). It is important to point out that any indication of such a mis-correspondence in the radial coordinate determination was not found applying the RS algorithm to simulated events [15]. Furthermore a similar effect was observed applying a genetic algorithm [18,19], a technique completely different from the RS, to the same set of data and using the same signal basis. These arguments indicate that the observed deviation is most likely due to a mis-correspondence between the calculated position response and real one in the detector middle/outer part confirming what was already pointed out in Refs. [18,19,41]).

In the case of the measurement performed at IKP Koln with the AGATA clusters, as a consistency check, a set of simulated events was produced by means of a dedicated GEANT-based code [42]. In the performed simulation 1381.7 keV γ-rays were emitted isotropically towards an AGATA detector from a point-like source positioned at a distance of 10 cm (i.e. target–detector distance in the experiment). The detector signals associated to each simulated event were calculated using the MGS [38] basis. These signals were then superimposed to real noise samples and folded with the response function of the pre-amplifier [22,35] and of the anti-aliasing filter [35]. The radial coordinate distribution resulting from the GEANT simulation is compared in Fig. 4 with that obtained following the application of the RS algorithm to the calculated signals produced from the same simulations. As expected the two curves match in an excellent way.

In Fig. 5 the simulated radial distribution (thick solid black line) and the one obtained applying the RS algorithm to the measured signals (empty black circles+thin solid black line) are compared. The distributions for segments lying in the same slice (for all the three crystals) are summed up in order to increase the counting statistics and thus minimizing statistical fluctuations. A general agreement between the distribution resulting from the

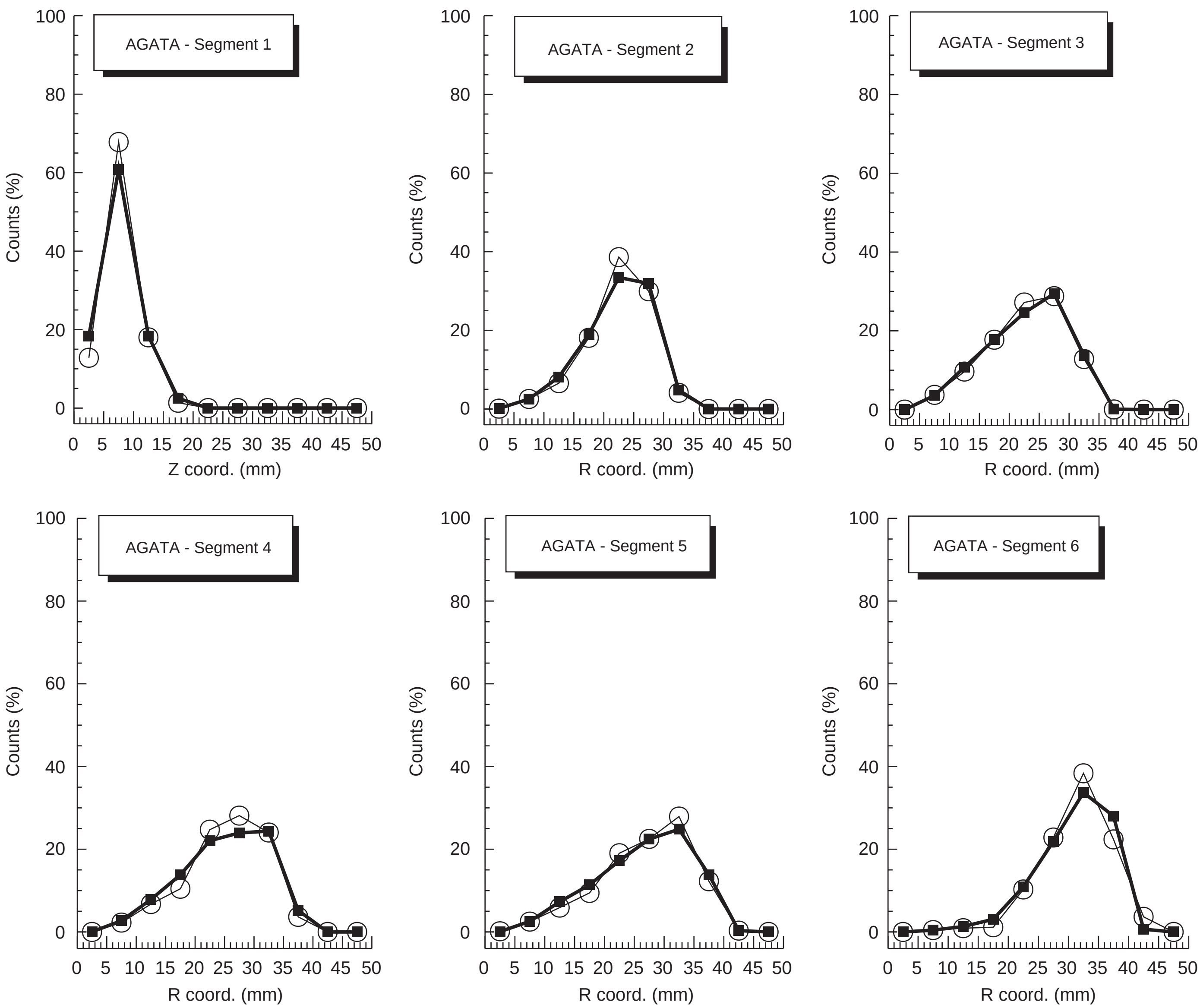

Fig. 4. The radial coordinate distributions of the gamma interactions obtained applying the RS algorithm to the simulated signals are displayed with empty black circles+thin solid black line. These are respectively compared with the expected distributions, obtained with a GEANT simulation (full black squares+thick solid black line). Each panel refers to a segment of a specific AGATA detector slice, starting from the detector front face (segment 1). The segment number is the same as that of Fig. 1. In all the plots the error bars are smaller than the symbol size.

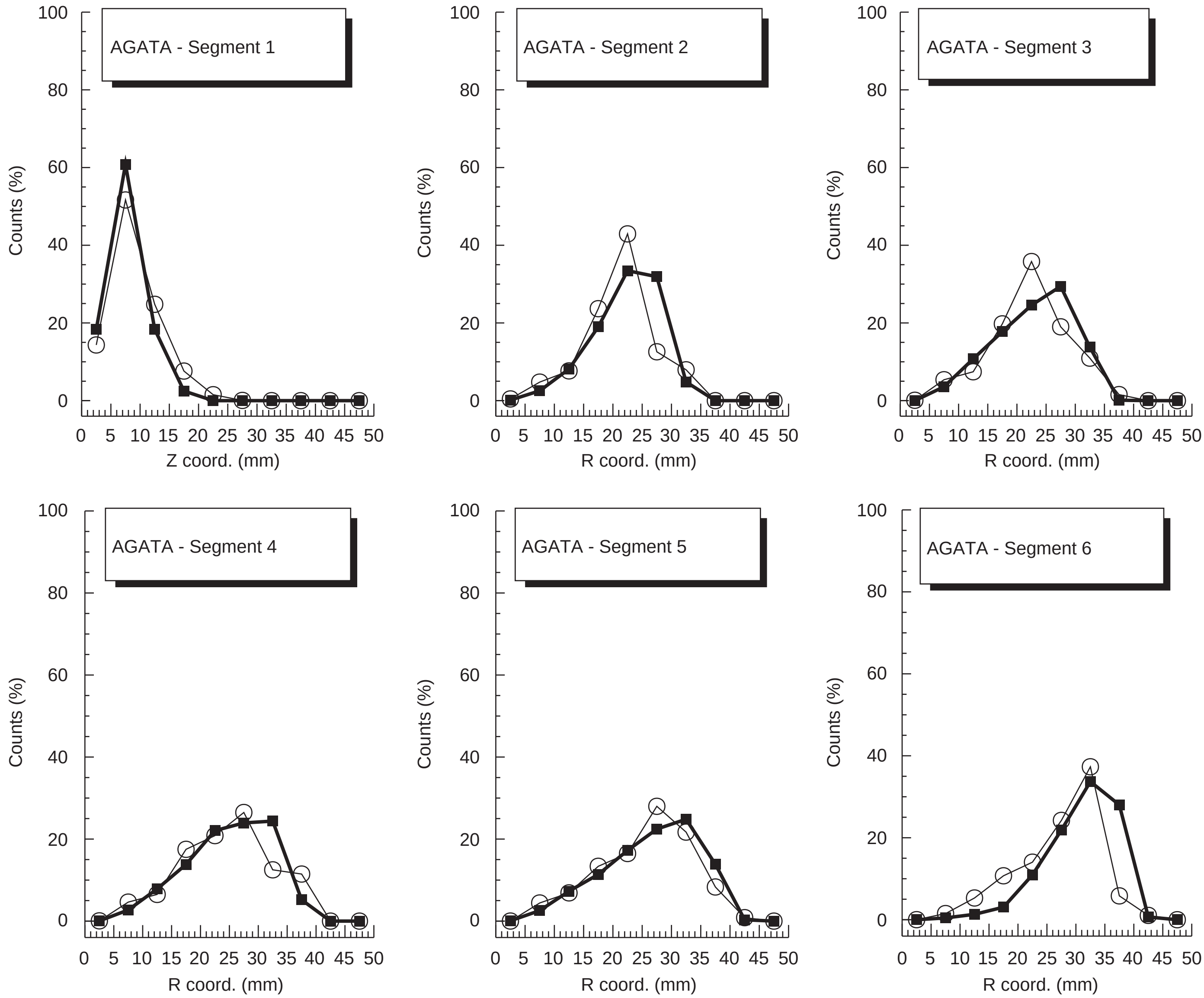

Fig. 5. The radial coordinate distributions of the gamma interactions obtained applying the RS algorithm to the experimental signals are displayed with empty black circles+thin solid black line. These are respectively compared with the expected distributions, obtained with a GEANT simulation (full black squares+thick solid black line). Each panel refers to a segment of a specific AGATA detector slice, starting from the detector front face (segment 1). The segment number is the same as that of Fig. 1. In all the plots the error bars are smaller than the symbol size.

GEANT simulation and that obtained applying the RS algorithm to the measured signals is evident in all panels even though some deviations are still present.

The excellent matching of the curves displayed in Fig. 4 strongly supports the fact that these deviations are not introduced by the RS algorithm; they can be attributed instead to a mis-correspondence between the calculated detector response and the real one, as in the case of the experiment with MARS detector.

However, it is evident that the mismatch for the distributions in Fig. 5 (AGATA detector case) is of minor importance with respect to the one of Fig. 3 (MARS detector case), reflecting the improvement in the quality of the calculations and in the understanding of HPGe segmented detectors functioning over the years (the MARS detector experiment was performed 4 years before than the AGATA one). The source of the mentioned residual mismatch could be adduced to the presence of cross talk effects between the different segments, which has been observed but not yet included in the calculations [43–45].

3.2. Number of interactions determination

The RS algorithm performances have been evaluated also by comparing the IPn distribution obtained applying the RS algorithm to the experimental signals with that resulting from GEANT simulations. In both experiments the IPn distribution was extracted from the same experimental dataset used to extract the radial distributions of Figs. 3 and 5 and the contributions associated to the different segments were summed up.

Figs. 6 and 7 show the IPn distributions obtained applying RS to the signals acquired in the two experiments described and respectively compared with those resulting from GEANT simulations. The experimental IPn distribution is displayed with empty black circles, the one resulting from the GEANT simulation with filled diamonds. In addition, in Fig. 7, the distribution obtained applying RS algorithm to the calculated signals has been added with empty black squares.

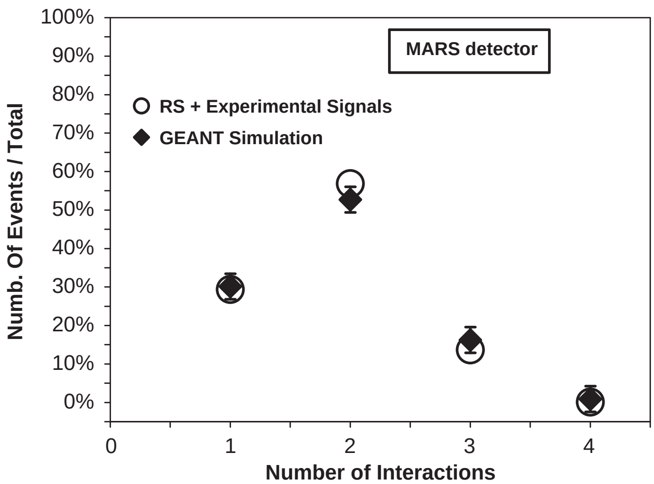

Fig. 6. The number of interaction per segment distribution obtained applying the RS algorithm to the experimental signals acquired during the MARS experiment is displayed with empty black circles. This is compared with the expected one, obtained with a GEANT simulation of the MARS experiment [40] (filled black diamonds). As can be seen, the two distributions match in an excellent way.

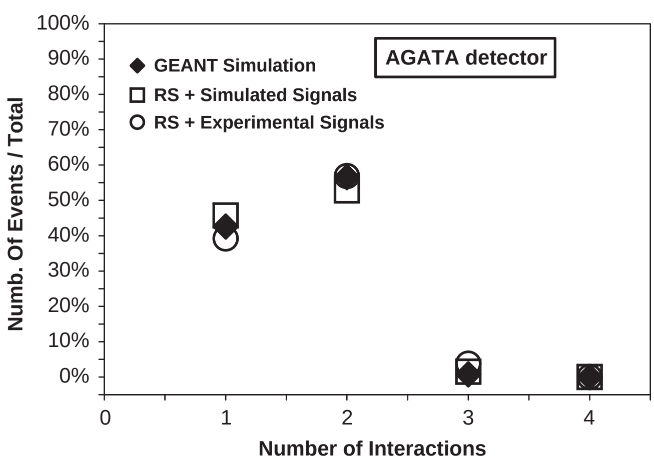

Fig. 7. The number of interaction per segment distribution obtained applying the RS algorithm to the experimental signals acquired during the AGATA experiment is displayed with empty black circles. This is compared with that obtained using the RS algorithm on simulated signals (empty black squares) and that calculated using a GEANT simulation. As can be seen, the agreement between the three distributions is excellent. The experimental events used to produce these plots have segment multiplicity that equals one. The error bars are smaller than the symbol size.

As can be observed, in both cases the experimental IPn distribution reproduces accurately the expected one. In general, we have found that, comparing the results of the RS algorithm (on simulated signals) with the original information from the GEANT simulation, in more than 80% of the cases both the IPn and the current pulse maxima position were properly identified.

The good agreement between simulations and data of Figs. 6 and 7 shows that it is possible to extract from the signals the numbers of IPs even when there is not a perfect matching between real signals and the calculated basis as shown in the previous section. This suggests also that the mismatch is not in the signal shape but most probably in its association to the position of the interaction inside the segment.

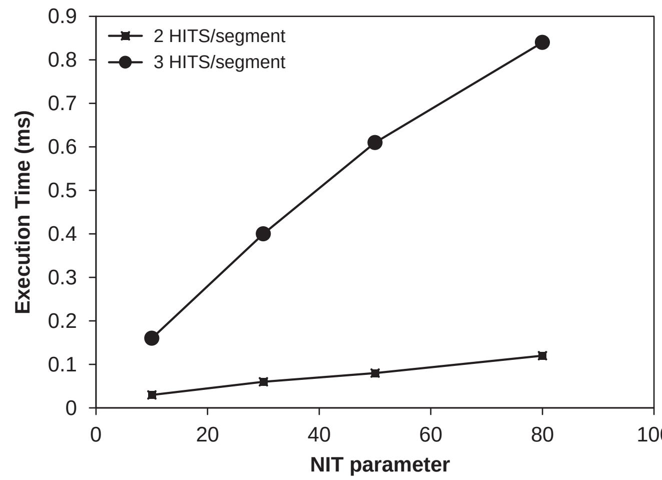

Fig. 8. The CPU time required by the RS algorithm to process one net charge signal plotted as a function of the NIT parameter. The two curves are related to the case of a number of interactions per segment limited to 2 (full black squares) and 3 (full black circles). The processor used is an Intel Xeon 3.2 GHz.

4. CPU requirements

As already stated in the Introduction, PSA algorithms must fulfill stringent CPU time constraints (i.e. <1 ms per event). In Fig. 8 the execution time performances of the RS algorithm are plotted as a function of the NIT parameter [15]. The two curves are associated to a maximum number of interactions per segment disentangled set to 2 (full black circles) and 3 (full black squares) [15,35]. The processor used is an Intel dual core (using one single Xeon 3.2 GHz) and the algorithm code (written in C) was compiled using the gcc-c++-4.1.2-33 compiler. It can be noted that in all the cases the execution time is below 1 ms. The value of the NIT parameter used for obtaining the previously shown results is 50 for both MARS and AGATA experimental signals.

5. Conclusion

The results of the application of RS algorithm to pulse shapes acquired during the in-beam tests of MARS and AGATA symmetric cluster detectors have been discussed. The algorithm performances have been evaluated by comparing the results obtained following its application to the experimental pulse shapes with that expected from GEANT simulations. Excellent agreement is found between the experimental distribution of the number of interaction per segment and the simulated one. Results on simulated signals indicate that the limit on the proper determination of the number of interactions is due to the fact that in some cases double interaction events and single interaction events are identical in shape; in particular this happens for nearly the 15% of the double interaction events (i.e. those for which the current pulse maxima superimpose). Furthermore, this number is consistent with the saturation in the algorithm performances for the determination of the number of interactions at about 85% (see Ref. [15]). Deviations between the experimental radial distribution of the interaction points and the simulated one have been found and we expect them to be associated to a mis-correspondence between the calculated detector position response and the real one. This is probably caused by the influence of cross talk on the detector signal shape, which is not taken into account in the used calculated response.

These results show the improvements in the understanding of the behaviour of HPGe segmented detectors. The experimental fact that deviations exist mainly for radial distributions evidences (i) the correctness of the signal shapes and a non-perfect matching between the signals and their localization inside the detector (ii) the importance of a correct understanding of cross talk [43–45]. Both effects could be accurately studied experimentally through a detailed scan of the detector, which could provide signal shapes from localized IPs in situations with and without cross talk [46–50]. The results here discussed are extremely encouraging in view of a complete and deep understanding of HPGe detectors for γ-ray tracking and imaging.

Acknowledgement

We acknowledge with thanks the fruitful discussion with Sebastiano Vigna from Dipartimento di Scienze dell'Informazione,Università di Milano, Italy.

References

[1] J. Simpson, Z. Phys. 358 (1997) 139.
[2] A. Deleplanque, R.M. Diamond, Lawrence Berkeley National Laboratory Report, 1988.
[3] J. Simpson, et al., Acta Phys. Hung. New Ser. Heavy Ion Phys. 11 (1–2) (2000) 159;
F. Azaiez, W. Korten, Nucl. Phys. News 7 (4) (1997) 21.
[4] 〈http://www.phys.jyu.fi/research/gamma/jurogam/〉.
[5] H.J. Wollersheim, Nucl. Instr. and Meth. A 537 (2005) 637.
[6] A. Gadea, et al., Eur. Phys. J. A 20 (2004) 193.
[7] D. Bazzacco, Nucl. Phys. A 746 (2004) 248C
J. Gerl, W. Korten (Eds.), AGATA Technical Proposal, September 2001, available at 〈http://www-w2k.gsi.de/agata/〉.
[8] C.W. Beausang, Nucl. Instr. and Meth. B 204 (2003) 666.
[9] R. Lieder, et al., Prog. Part. Nucl. Phys. 46 (2001) 399.
[10] Y. Lee, et al., Rep. Prog. Phys. 66 (2003) 1095.
[11] O. Wieland, et al., IEEE Trans. Nucl. Sci. NS-48 (3) (2001).
[12] G.J. Schmidt, et al., Nucl. Instr. and Meth. A 430 (1999) 69.
[13] J. van der Marel, B. Cederwall, Nucl. Instr. and Meth. A 437 (1999) 538.
[14] O. Wieland, et al., Nucl. Instr. and Meth. A 487 (2002) 441.
[15] F.C.L. Crespi, Nucl. Instr. and Meth. A 570 (2007) 459.
[16] A. Olariou, P. Desesquelles, et al., IEEE Trans. Nucl. Sci. NS-53(1) (3) (2006) 1028.
[17] Th. Kröll, D. Bazzacco, Nucl. Instr. and Meth. A 565 (2006) 691.
[18] Th. Kröll, et al., Nucl. Instr. and Meth. A 586 (2008) 421.
[19] M. Nespolo, Ph.D Thesis, University of Padova, Italy, 2004, available at 〈http://npgroup.pd.infn.it/archivioTesi.htm〉.
[20] F. Recchia, Acta Phys. Pol. B 38 (2007).
[21] F. Recchia, Ph.D Thesis, University of Padova, Italy, 2008.
[22] M. Schlarb, Presentations at the AGATA week November 12–15, 2007-INFN, Laboratori Nazionali di Legnaro—Italy and at AGATA week January 15–19, IPNO and CSNSM laboratories of the IN2P3 institution at the University of Orsay. website: 〈http://www.e12.physik.tu-muenchen.de/AGATA/〉 and 〈http://www-w2k.gsi.de/agata/〉.
[23] R. Venturelli, D. Bazzacco, LNL-INFN(REP)—204 (2005) 220.
[24] D.C. Radford, Signal Decomposition Algorithm for GRETINA, AGATA week GSI 2005, available at 〈http://npg.dl.ac.uk/AGATA/agata_week_talks/〉.
[25] K. Vetter, et al., Nucl. Phys. A 682 (2001) 286C.
[26] K. Vetter, et al., Nucl. Instr. and Meth. A 452 (2000) 105.
[27] K. Vetter, et al., Nucl. Instr. and Meth. A 452 (2000) 223.
[28] I. Doxas, et al., Nucl. Instr. and Meth. A 580 (2007) 1331.
[29] M. Descovich, et al., Nucl. Instr. and Meth. A 553 (2005) 535.
[30] A. Khaplanov, et al., Nucl. Instr. and Meth. A 580 (2007) 1075.
[31] K. Vetter, et al., Nucl. Instr. and Meth. A 579 (2007) 363.
[32] R.J. Cooper, et al., Nucl. Instr. and Meth. A 579 (2007) 313.
[33] T. Niedermayr, et al., Nucl. Instr. and Meth. A 553 (2005) 501.
[34] F. Recchia, D. Bazzacco, E. Farnea, R. Venturelli, S. Aydin, G. Suliman, C.A. Ur, Nucl. Instr. and Meth. A (2009).
[35] F.C.L. Crespi, Ph.D Thesis, University of Milano, Italy, 2008.
[36] R. Venturelli, et al., LNL Annual Report 2002, INFN-LNL(REP)198/2003, pp. 154–156.
[37] H.G. Essel, et al., IEEE Trans. Nucl. Sci. NS-43 (1) (1996) 132.
[38] P. Medina, et al., A Simple Method for the Characterization of HPGe Detectors, IMTC 2004, Como, Italy, website: 〈http://mgs2005.in2p3.fr/Mgs.php〉.
[39] 〈http://www-win.gsi.de/agata/〉.
[40] M. Nespolo, Private communication.
[41] F.C.L. Crespi, et al., Acta Phys. Pol. B 38 (2007).
[42] E. Farnea, D. Bazzacco, LNL-INFN(REP)—202 (2004) 158 website: 〈http://agata.pd.infn.it〉.
[43] Bart Bruyneel, et al., Nucl. Instr. and Meth. A 599 (2009) 196.
[44] B. Bruyneel, Ph.D. Thesis, Institut fur Kernphysik, Universitat zu Koln.
[45] M. Dimmok, B. Bruyneel, Presentation at Agata week Uppsala—website: 〈http://www-w2k.gsi.de/agata/〉.
[46] A. Boston, et al., Nucl. Instr. and Meth. B 261 (2007) 1098.
[47] K. Vetter, et al., Nucl. Instr. and Meth. A 452 (2000) 223.
[48] I. Kojouharov, S. Tashenov, T. Engert, J. Gerl, H. Schaffner, IEEE Nucl. Sci. Symp. Conf. Rec. 3 (2007) 2213 〈http://www-w2k.gsi.de/agata/〉.
[49] A. Korichi, M.-H. Ha, Presentations at the AGATA week November 12–15, 2007-INFN, Laboratori Nazionali di Legnaro, Italy. AGATA week January 15–19, IPNO and CSNSM laboratories of the IN2P3 institution at the University of Orsay 〈http://www-w2k.gsi.de/agata/〉.
[50] F.C.L. Crespi, et al., Nucl. Instr. and Meth. A 593 (2008) 440.